

TRACKING VORTICES OVER LARGE DISTANCES USING VORTICITY CONFINEMENT

Rainald Löhner and Chi Yang

School of Computational Sciences
M.S. 4C7, George Mason University, Fairfax, VA 22030-4444, USA

ABSTRACT

A general vorticity confinement term has been derived using dimensional analysis. The resulting vorticity confinement is a function of the local vorticity-based Reynolds-number, the local element size, the vorticity and the gradient of the absolute value of the vorticity. The vorticity confinement term disappears for vanishing mesh size, and is applicable to unstructured grids with large element size disparity. The new term has been found to be successful for a number of testcases, allowing better definition of vortices without any deleterious effects on the flowfield.

Keywords: Vorticity Confiement, Vortical Fow, CFD, Unstructured Grids

1. INTRODUCTION

The requirement to accurately track vortices over large distances is common to many areas of engineering, e.g. rotating helicopter blades [Ca00, St00] and vortices shed by submarines. Due to the inherent dissipation built into numerical flux functions in order to avoid numerical instabilities and unphysical solutions, any current Euler or RANS field solver will tend to dissipate these vortices too fast. In order to obtain a rough estimate for the grid sizes required to capture accurately typical trailing edges vortices, consider a helicopter blade with radius $r = 5m$ and a vortex of size $\delta = 10cm$. The element size required to describe such a vortex will be smaller than $h = 1cm$ (10 elements across the vortex zone). The volume occupied by the vortex per blade rotation is approximately

$$V_\omega = \pi \cdot 10^2 cm^2 \cdot 2\pi \cdot 5 \cdot 10^2 cm \approx 10^6 cm^3 \quad .$$

Given that the vortex is moving, and possibly interacting with blades and other vortices, an isotropic grid seems prudent. Such a grid would require at least 10^6 points per blade rotation. This should be viewed as a lower limit, as the only free parameter is the mesh size, which, in all likelihood, was estimated too large. Similarly, estimates for the number of gridpoints required to track accurately one or more vortices for one submarine length easily approach billions of points, making such calculations impractical for the next decade (if Moore's law continues). In order to avoid the rapid dissipation of

vortices, Steinhoff and co-workers have introduced the concept of vorticity confinement [St94, St99, Hu00], refining it over the last decade and applying it successfully to a number of relevant flows [Mo00]. The basic technique consists of adding a force-term to the momentum equations, resulting in:

$$\rho \mathbf{v}_{,t} + \rho \mathbf{v} \nabla \mathbf{v} + \nabla p = \nabla \mu \nabla \mathbf{v} - \epsilon \rho \mathbf{n} \times \boldsymbol{\omega} \quad , \quad (1)$$

where ρ , \mathbf{v} , p , μ and $\boldsymbol{\omega}$ denote, respectively, the density, velocity, pressure, viscosity and vorticity of the fluid, ϵ a user-defined number and \mathbf{n} is a ‘normal’ vector. Note that this additional force acts in the direction normal to the vorticity and \mathbf{n} , thus convecting vorticity back towards the centroid as it diffuses away. A typical choice for \mathbf{n} is:

$$\mathbf{n} = \frac{\nabla |\boldsymbol{\omega}|}{|\nabla |\boldsymbol{\omega}||} \quad . \quad (2)$$

Steinhoff and co-workers [St94, St99, Hu00, Mo00] were able to demonstrate that vortices could be captured and maintained for long distances without dissipation. Steinhoff and co-workers have worked mainly on uniform Cartesian grids, for which ϵ could be kept constant. Murayama [Mu01] attempted to use this type of vorticity confinement on an unstructured grid, i.e. leaving ϵ constant. The results were mixed. For some values of ϵ , an improvement of results was observed. Other values of ϵ lead to unphysical results, e.g. premature vortex burst on a delta wing. These results make it clear that for non-uniform grids a general solution has to be found. Vorticity confinement has also been used recently for the visual simulation of smoke [Fe01]. These animations were performed on Cartesian grids using the incompressible Navier-Stokes equations, and included (for the first time, to the author’s knowledge) an explicit, linear dependence on the mesh size h .

2. DIMENSIONAL ANALYSIS

From dimensional analysis, one can see that ϵ must have the dimension of a velocity. One could either use $|\mathbf{v}|$, $h|\boldsymbol{\omega}|$ or $h^2|\nabla|\boldsymbol{\omega}||$. Considering Eqn.(2), the last form is particularly appealing, leading to:

$$\rho \mathbf{v}_{,t} + \rho \mathbf{v} \nabla \mathbf{v} + \nabla p = \nabla \mu \nabla \mathbf{v} - c_1 \rho h^2 \nabla |\boldsymbol{\omega}| \times \boldsymbol{\omega} \quad , \quad (3)$$

where c_1 is now a true constant, regardless of the grid. One can see immediately that the vorticity confinement term is of the form of an anti-diffusion, and that it will disappear as the grid gets finer and finer ($h \rightarrow 0$).

3. PROPER LENGTH SCALE h

A crucial ingredient in the vorticity confinement given by Eqn.(3) is the length scale h . It was found that for isotropic grids, most of the possible forms: average of edge-lengths surrounding a point, volume to surface ratio of elements surrounding a point,

etc., gave similar results. As expected, the situation is markedly different for highly stretched grids. Here, it was found that taking h as the characteristic length in the direction of $\nabla|\omega|$ was the proper choice. The determination of characteristic lengths in the x, y, z directions is performed by observing that the gradient, computed as:

$$g_k^i = M_l^i \cdot \sum_{ij} C_k^{ij} (u_i + u_j) \quad (4)$$

for point i , direction k and edges i, j surrounding point i , will be of dimension $[[u]/[h]]$. Therefore, an approximate estimate for the characteristic element length in direction k may be obtained from:

$$(h_k^i)^{-1} = 2M_l^i \cdot \sum_{ij} |C_k^{ij}| \quad (5)$$

Denoting by \mathbf{h} the characteristic element lengths computed, the final form of h is given by:

$$h = \mathbf{h} \cdot \frac{\nabla|\omega|}{|\nabla|\omega||} \quad (6)$$

4. TREATMENT OF BOUNDARY LAYERS

The primary function of vorticity confinement is to enhance the capture of relevant physics in regions where mesh density is insufficient. This is not the case in well resolved boundary layers close to solid surfaces. In fact, it was found that switching on vorticity confinement in these highly resolved regions could lead to numerical instabilities. Therefore, an explicit switch, based on the local Reynolds-number Re_h , was attempted:

$$h_v = \min(1, Re_h) \cdot h \quad ; \quad Re_h = \frac{\rho v h}{\mu} \quad (7)$$

This form did not prove satisfactory. A more universal form, that is tied to the terms used for vorticity confinement, is a local Reynolds-number defined with the vorticity. From dimensional analysis, one may observe that the following three candidates could be used:

$$Re_{\omega,h} = \frac{\rho|\Delta v|h}{\mu} \quad ; \quad Re_{\omega,h} = \frac{\rho|\omega|h^2}{\mu} \quad ; \quad Re_{\omega,h} = \frac{\rho|\nabla|\omega||h^3}{\mu} \quad (8)$$

The final form of the vorticity confinement force then takes the form:

$$\mathbf{f} = g(Re_{\omega,h})c_1\rho h^2\nabla|\omega| \times \omega \quad ; \quad g = \max \left[0, \min \left[1, \frac{Re_{\omega,h} - Re_{\omega,h}^0}{Re_{\omega,h}^1 - Re_{\omega,h}^0} \right] \right] \quad (9)$$

5. NUMERICAL RESULTS

The vorticity confinement described above was implemented into FEFLO, a general adaptive unstructured finite element flow solver [Lö01]. The results shown were all obtained by using a projection-type incompressible flow solver [Lö98] that employs a second-order upwind advection operator and a fourth-order pressure damping for the divergence constraint [Lö99].

5.1 NACA0012 (Euler): The first case considered is that of a finite width NACA0012 wing, characteristic of control surfaces.

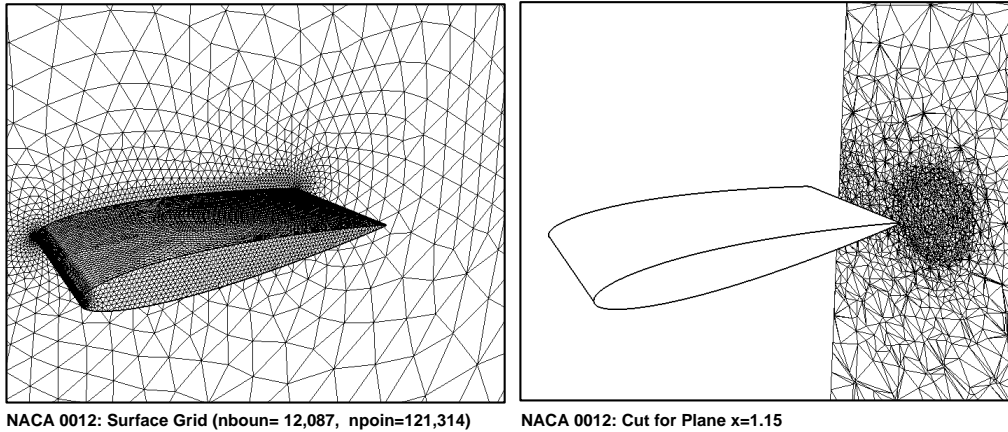


Figure 1a,b NACA0012: Surface Mesh and Cut Plane $x = 1.15$

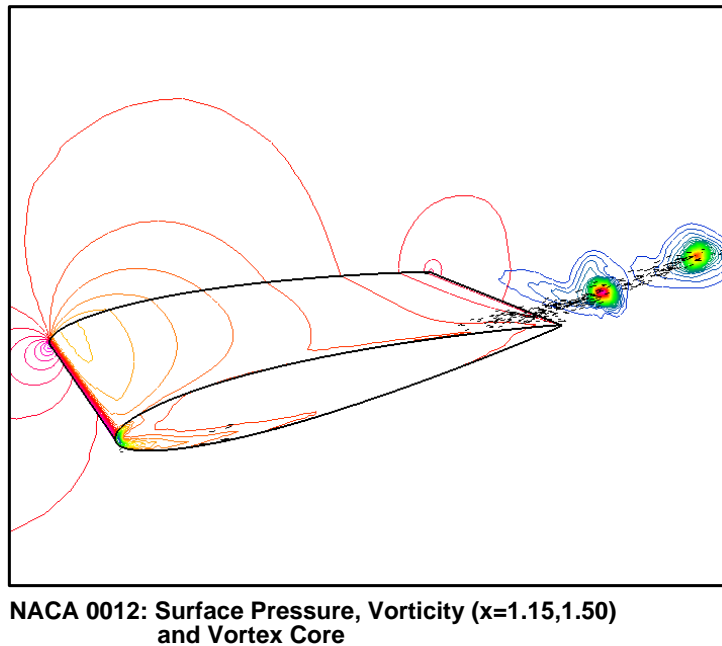
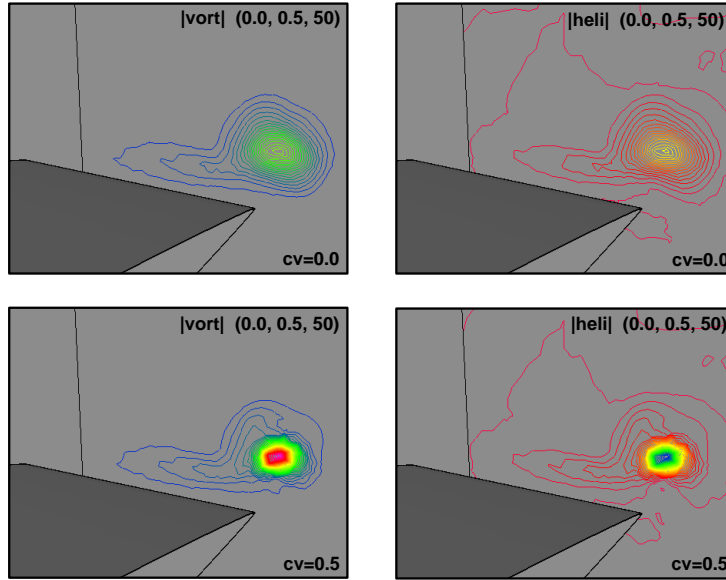


Figure 1c Finite NACA0012 Wing

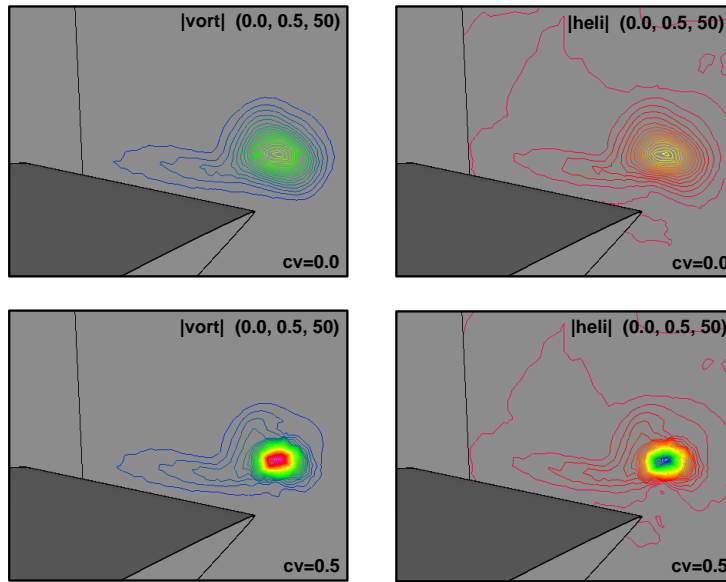
The incompressible Euler equations are solved for an angle of attack of $\alpha = 15^\circ$.

Figures 1a,b show the surface mesh employed, as well as a cut normal to the x-direction at 15% chord length downstream of the trailing edge. Note that a line-source was specified in the approximate position of the vortex in order to obtain a finer grid. The mesh had approximately 120,000 points, with 12,000 points on the boundary.



NACA 0012: Comparison of Vorticity and Helicity at $x=1.15$

Figure 1d Finite NACA0012 Wing: Comparison of Vorticity and Helicity



NACA 0012: Comparison of Vorticity and Helicity at $x=1.15$

Figure 1e Finite NACA0012 Wing: Comparison of Vorticity and Helicity

Figure 1c shows the results with the vorticity confinement terms switched on. The

vortex core visualization shows how well the vortex is captured. Figures 1d,e compare the vorticity and helicity ($\mathbf{v} \cdot \boldsymbol{\omega}$) in two planes downstream of the wing. The effect of vorticity confinement is clearly visible. Without vorticity confinement, the vortex is dissipated after only one chord length of the airfoil.

5.2 Delta Wing (Laminar NS): The second case considered is that of the delta-wing measured by Hummel [Hu67] and computed by Murayama [Mu01]. This is a laminar case, making it ideally suited for benchmarking. The angle of attack is $\alpha = 20.5^\circ$, and the Reynolds-number based on the length of the wing is $Re = 10^6$. The grid, shown in Figures 2a,b, is typical of RANS calculations. In the proximity of the wall, the elements are highly anisotropic with extremely fine spacing normal to the wall. Away from the wall the mesh coarsens rapidly and becomes isotropic. The primary vortex generated by the delta wing rapidly enters regions of low mesh density. Figure 2c shows the vorticity and pressure contours for planes located at 30%, 50% and 70% root chord length for the case with vorticity confinement switched on. The vortex strength for the 50% chord plane are compared in Figure 2d. As before, vorticity confinement has a marked effect on the strength of the detached vortex.

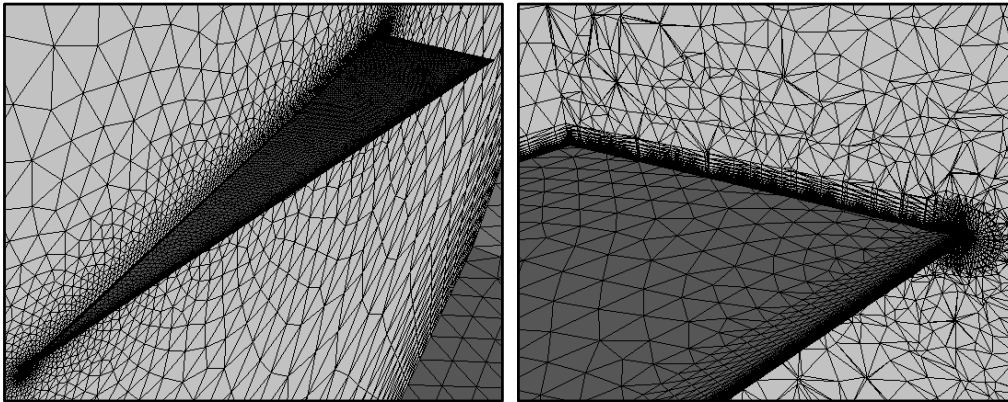


Figure 2a,b Delta-Wing: Surface Mesh and Detail

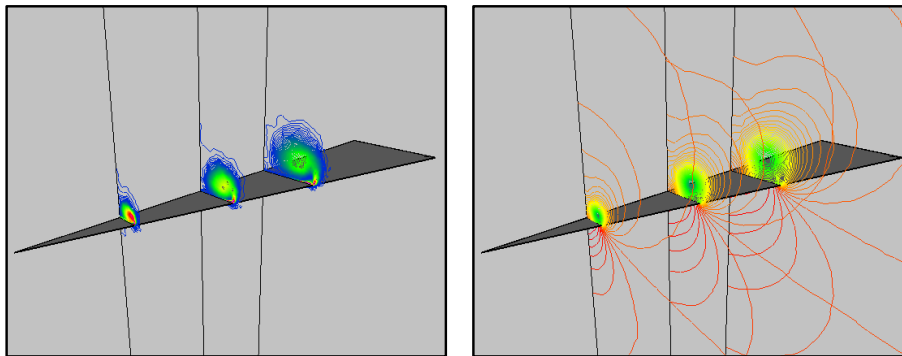
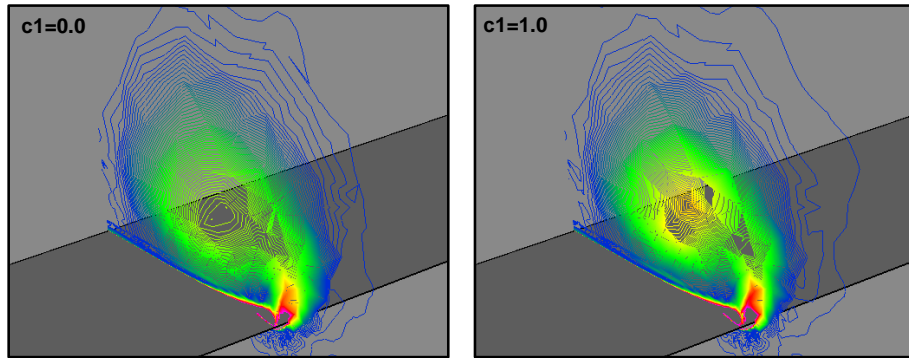


Figure 2c Delta-Wing: Vorticity and Pressure in Planes $x = 0.3, 0.5, 0.7$

Figure 2d Delta-Wing: Comparison of Vorticity for Plane $x = 0.5$

6. CONCLUSIONS AND OUTLOOK

A general vorticity confinement term for unstructured grids has been derived, implemented and found to be successful for some cases. The vorticity confinement terms are of the form:

$$\mathbf{f} = g(Re_{\omega,h})c_1\rho h^2\nabla|\omega| \times \omega \quad ,$$

where $c_1 = O(1)$, h is a characteristic element size and g depends on the local vorticity-based Reynolds-number $Re_{\omega,h}$.

We are currently investigating in more depth the theoretical aspects associated with vorticity confinement. In particular:

- One can see that the vorticity confinement as given by Eqn.(3) is in the form of a body force. As such, these terms may add or subtract axial and/or tangential moment from the surrounding flow. We are attempting to derive hard estimates/proofs for the axial and tangential moment attributed to vorticity confinement. Our present conjecture of that such estimates can be obtained by making use of Stokes' theorem for vorticity.
- It is possible that the vorticity confinement terms introduce errors in the flowfield. For benchmark problems (e.g. delta wing), more tests are required to determine the source of errors and to quantify them.
- Finally, other formulations for vorticity are certainly possible.

7. ACKNOWLEDGEMENTS

This research was partially supported by ONR, with Dr. Patrick Purtell as the technical monitor.

8. REFERENCES

- [Ca00] F. Caradonna - Developments and Challenges in Rotorcraft Aerodynamics; *AIAA-00-0109* (2000).
- [Fe01] R. Fedkiw, J. Stam and H.W. Jensen - Visual Simulation of Smoke; pp. 15-22 in *Proc. SIGGRAPH 2001*, Los Angeles, CA (2001).
- [Hu67] D. Hummel and P.S. Srinivasan - Vortex Breakdown Effects on the Low-Speed Aerodynamic Characteristics of Slender Delta Wings in Symmetrical Flow; *Royal Aeronautical Society Journal* 71, 319-322 (1967).
- [Hu00] G. Hu, B. Grossman and J. Steinhoff - A Numerical Method for Vortex Confinement in Compressible Flow; *AIAA-00-0281* (2000).
- [Lö98] R. Löhner, C. Yang and E. Oñate - Viscous Free Surface Hydrodynamics Using Unstructured Grids; *Proc. 22nd Symp. Naval Hydrodynamics*, Washington, D.C., August (1998).
- [Lö99] R. Löhner, Chi Yang, E. Oñate and S. Idelsohn - An Unstructured Grid-Based, Parallel Free Surface Solver; *Appl. Num. Math.* 31, 271-293 (1999).
- [Lö01] R. Löhner - FEFLO User's Manual; *GMU-CSI/CFD-01-01* (2001).
- [Mo00] M. Moulton and J. Steinhoff - A Technique for the Simulation of Stall with Coarse-Grid CFD; *AIAA-00-0277* (2000).
- [Mu01] M. Murayama, K. Nakahashi and S. Obayashi - Numerical Simulation of Vortical Flows Using Vorticity Confinement Coupled With Unstructured Grid; *AIAA-01-0606* (2001).
- [St94] J. Steinhoff - Vorticity Confinement: A New Technique for Computing Vortex Dominated Flows; pp. 235-263 in *Frontiers of Computational Fluid Dynamics* (D.A. Caughey and M.M. Hafez eds.), J. Wiley & Sons (1994).
- [St99] J. Steinhoff, W. Yonghu and W. Lesong - Efficient Computation of Separating High Reynolds Number Incompressible Flows Using Vorticity Confinement; *AIAA-99-3316-CP* (1999).
- [St00] R. Strawn - Computational Modeling of Hovering Rotors and Wakes; *AIAA-00-0110* (2000).